CHEMICAL ENGINEERING TRANSACTIONS
VOL. 108, 2024
A publication of AIDIC
The Italian Association of Chemical Engineering
Online at www.cetjournal.it
Guest Editors: Carlo Pirola, Antonio Espuña
Copyright © 2024, AIDIC Servizi S.r.l.
ISBN 979-12-81206-08-3; **ISSN** 2283-9216
DOI: 10.3303/CET24108004

Use of Activated Carbon from the Seed of Persea Americana (var Hass) in the Removal of Mercury (Hg^{2+}) from Wastewater

John R. Castro-Suarez[a*], Arnulfo Tarón-Dunoyer[b*], Fredy Colpas-Castillo[c]

[a]Exact Basics Area, Campus Cartagena, University of Sinú-Elías Bechara Zainúm, Cartagena 130001, Colombia
[b]GIBAE Research Group, Faculty of Engineering, University of Cartagena, Cartagena 130015, Colombia
[c]Carbochemistry Research Group, Faculty of Exact and Natural Sciences, University of Cartagena, Cartagena 130015.
johncastrosuarez@gmail.com, atarond@unicartagena.edu.co

This work aimed to study the removal of mercury from industrial wastewater, using activated carbon from Hass avocado seed. The seed was carbonized to obtain activated carbon. Orthophosphoric acid at 21% w/v was used as an activating agent. The Hg^{2+} concentration was determined by atomic absorption spectroscopy. The chemical surface of the material was performed by Fourier transform infrared spectroscopy. The carbons were morphologically characterized using a scanning electron microscope. The conditions of the experiments were 50 mL of industrial wastewater at room temperature, pH 6.0, initial concentration of mercury 0.036 mgL^{-1} and 0.2 gL^{-1} of adsorbent material. The average removal efficiency of activated carbon (CA) for Hg^{2+} was 84% and an equilibrium concentration of 0.006 mgL^{-1} after 60 minutes. Two kinetic models and one diffusion model were applied. The model that best describes the adsorption process was the Elovich model with an R^2 of 0.9897. Results show that the seed of Persea americana is useful for obtaining carbon and becomes a good alternative to use in industrial wastewater treatments for the removal of Hg^{2+}, turbidity, color, and total solids.

1. Introduction

The rapid development of industrial and urban activities adds large amounts of industrial waste and potentially toxic elements, causing great pollution risk to aquatic ecosystems and causing many serious environmental and health problems for humans (Gheitasi et al., 2022).Heavy metals such as mercury, cadmium, lead, nickel, chromium, and zinc are considered very dangerous because they are non-biodegradable and have a toxic and carcinogenic nature (Liu et al., 2020). Among heavy metals, mercury is a highly toxic metal even in small amounts (Chen et al, 2019). Its physical properties at room temperature allowed the use of mercury for various industrial purposes in medicine, dentistry, the military industry, and mining, among others (Gluszcz et al., 2008). Introduced into the natural environment regardless of its form, it can be relatively easily converted into highly toxic soluble and volatile forms, ie methyl chloride or ethyl mercury, which are much more bioavailable and much more toxic than other forms of mercury. Furthermore, mercury is largely retained in living organisms and thus biomagnifies, primarily through the aquatic food chain. (Boenign, 2000).
Due to the issues posed by this element, several methods have been employed to eliminate it from aqueous media. Among these methods, adsorption on active materials such as activated carbon (CA) or ion exchange resins (Chiarle et al., 2000) has emerged as one of the most widely used approaches for water and wastewater treatment. It offers a simple and effective means for removing heavy metal ions, particularly in low and medium concentrations, without involving chemical reactions, thus garnering the attention of numerous researchers (Samad et al., 2019; Lahreche et al., 2022)
However, finding the most efficient adsorbent is difficult since the selection process needs the availability of residues (Samad et al., 2019). In fact, the factors of cost, space, and the amount of wastewater that affect the applicability of the adsorption method should also be thoroughly considered when it comes to an industrial application. CA derived from lignocellulose materials prepared by the chemical activation method often exhibit higher S_{BET} and V_{total} parameters than those of the physical activation method. Several chemical activating agents used for the chemical activation process have been reported such as $ZnCl_2$, KOH, H_3PO_4, $Fe_2(SO_4)_3$ among others (Ruiz-Fernández et al., 2011).

Paper Received: 05 August 2023 ; Revised: 26 November 2023 ; Accepted: 19 January 2024
Please cite this article as: Castro-Suarez J.R., Taron-Dunoye A., Colpas-Castillo F., 2024, Use of Activated Carbon from the Seed of Persea Americana (var Hass) in the Removal of Mercury (Hg2+) from Wastewater, Chemical Engineering Transactions, 108, 19-24 DOI:10.3303/CET24108004

Therefore, this study aims to investigate the removal efficiency of Hg^{2+} ions in a sample of industrial wastewater from fishing industries, using CA from Hass Avocado seed (Persea americana "Hass"), obtained by using the one-stage chemical activation method. The evaluation was carried out under conditions of pH 6, contact time 60 minutes, adsorbent dose 0.2 g, and initial concentration of mercury (II) ions 0.36 mgL^{-1}.

2. Materials and methods

2.1 Obtaining the non-active adsorbent material (CNA).

Persea americana "Hass" avocado seed was used as plant material, which was acquired in the market local. The seeds were dried in a conventional oven at 105ºC/4h and mechanically crushed to facilitate their carbonization process. Then,100 g of dry *Persea americana* "Hass" seed were taken and subjected to carbonization at a heating rate of 10ºC/min up to 350ºC in a Terrigeno clay oven, model DB 1200. The charcoal obtained was passed through a standard Tyler sieve #40 mesh.

2.2 Chemical activation of carbon.

The charred fractions were impregnated with a 21% (w/v) orthophosphoric acid solution for 5 hours with constant stirring. They were then dried at 110 °C/24h. Subsequently, the dry material was heated under a nitrogen atmosphere (flow rate of 110 mL/min) at a heating rate of 10ºC/min, up to 405ºC. Finally, the samples were washed with enough hot and cold water to obtain a conductivity value in the wash water between 0.5 and 5 µS/cm, with pH around 6.5.

2.3 Characterization of the adsorbent material (CA)

2.3.1. Particle size and specific area

Particle size and specific area were determined using the Mastersizer 3000 laser diffraction particle size analyzer (Malvern Instruments Ltd., Malvern, Worcestershire, United Kingdom, with velocity 10 kHz data acquisition and measurement time < 10 s.

2.3.2. Chemical Surface Study

The chemical surface of the activated (CA) and non-activated (CNA) adsorbent material was analyzed using Fourier transform infrared spectroscopy (FTIR). Spectra were obtained using the Nicolet iS50 FTIR equipment. Spectral range 400 – 4000 cm^{-1}. Spectral resolution 4 cm^{-1}.

2.3.3. Morphological characterization of the adsorbent material

The morphological characterization of the adsorbent material was performed by scanning electron microscopy (SEM), using a scanning electron microscope (Jeol 5910LV), with a voltage of 15Kv. Before being observed by SEM, the samples were subjected to a vacuum and then coated with a thin layer of gold to better visualize the electrons that distribute the intensity of the signals in the observation.

2.4 Adsorption kinetics

According to Attari et al. (2017), the adsorption mechanism is affected by the adsorbate and adsorbent characteristics and their interaction through contact time. To evaluate the Hg^{2+} elimination mechanism, the Elovich kinetic models, the intraparticle diffusion model, and the pseudo-second-order model were used by CA (Boparai et al., 2011; Gupta and Bhattacharyya, 2011; Robati, 2013).

2.5 Adsorption of Hg^{2+} on activated carbon

0.2 g of activated carbon (CA) was added to a 50 mL sample of the residual water, with continuous stirring at room temperature for 60 minutes. Subsequently, it was filtered, and the residual mercury (Hg^{2+}) was determined by atomic absorption spectroscopy (AA), in a Thermo Scientific iCE 3300 equipment. The concentration of mercury in the residual water before and after treatment with the adsorbent material (CA) is referred to as a calibration curve of a certified mercury concentration standard of 1000 mg/L (Merck) prepared at different concentrations.

2.6 Statistical analysis

The data obtained were statistically analyzed using a T-test. The MINITAB computer program was used to establish significant statistical differences at a significance level of 95%, between the values of the physicochemical parameters, before and after treatment with the adsorbent.

3. Results and Discussion

3.1 Specific areas of the CA

The specific surface area of the non-activated carbon was 76.86 m²/kg and after the activation and sieving process, a carbon with a specific surface area of 203.2 m²/kg was obtained, which indicates that the activation processes of carbon manage to significantly increase the area by 264.3%. However, this area is much smaller than that reported by Liu et al. (2020) for carbon from corn cob by KOH activation, which ensures lower adsorption rates.

3.2 Study of the chemical surface of the adsorbent material (CA)

FTIR spectroscopy provides insights into the material's functional groups. The presence of diverse functional groups in activated carbon (CA) is evident from the distinct bands observed in its spectra when compared with non-activated carbon (CNA). Figure 1 shows the IR spectrum corresponding to the CA and CNA samples, showing a band with a marked intensity approximately at 3450 cm^{-1}, which corresponds to the stretching vibration of the OH group present on the surface of activated carbon. The spectrum also shows the presence of other functional groups such as carbonyls C=O that are in the 1659 cm^{-1} band of CA. In addition, the C-O is identified in 1100 - 1000 cm^{-1}, which presents acid characteristics to the adsorbent material (Bibi et al., 2023).
It should be noted that the OH functional group is the most representative in the samples, both activated and non-activated, and something very particular in this group is that by forming hydrogen bonds, the adsorption frequencies multiply and allow all of them to overlap in a band, influencing that it can react with metal ions or other compounds present in the material and thus initiate its elimination process through its amphoteric characteristic (Rojas-Morales et al., 2016). Other bonds are also observed, such as P=O, and P-O-C that are found by impregnation of the activating agent. Finally, the FTIR characterization of activated carbon showed that activation with orthophosphoric acid strongly modifies the surface.

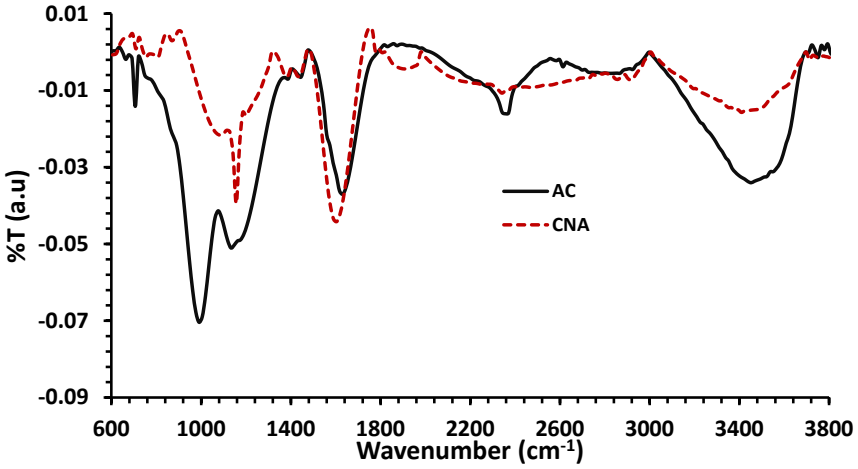

Figure 1: FTIR spectrum of activated carbon and unactivated carbon from Persea americana seed.

3.3 Morphology by scanning electron microscopy (SEM).

Figure 2 exhibits scanning electron microscopy images of activated and unactivated carbon derived from the seed of Persea americana "Hass" at varying magnifications. Figures 2c-d demonstrate an irregular and diverse structure, indicating the porous nature of the activated carbon. In contrast, the unactivated carbon (figures 2a-b) lacks these features and exhibits a broader size range, ranging from 30.1 to 83.10 µm, which surpasses the irregular sizes of CA that range between 16.2 and 55.98 µm. It is worth noting that smaller carbon sizes result in higher adsorption capacity due to increased contact surfaces between carbon particles.
Within this context, some micrometric granules of CA and CNA derived from biomass, not forming part of the carbon walls, can be observed. This dispersion is attributed to the activating agent or the crushing process of Persea americana "Hass" seeds (Viera and Cruz, 2019).
According to Rojas-Morales (2016), the activating agent H_3PO_4 induces a dehydration process during activation, preventing the formation of tar or any liquid that might block the sample's pores. This allows for improved movement of volatiles through the pore ducts without obstruction, leading to their release from the carbon surface during the activation process. Consequently, after the material is removed, it remains expanded, creating a sufficiently porous structure.

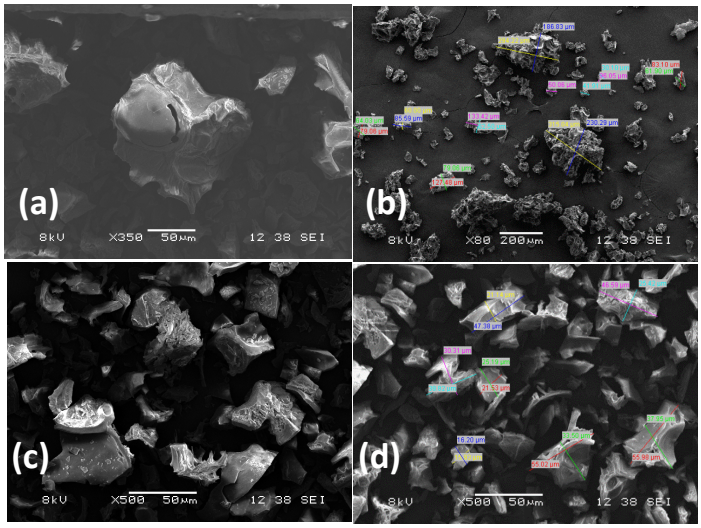

Figure 2: SEM images at different magnifications of persea americana seed carbon. (a) y (b) SEM images for CNA. (c) y (d) SEM images for CA.

3.4 Mercury removal

Industrial wastewater from a fishing industry company located in the city of Cartagena de Indias - Colombia was used as the sample. The wastewater was characterized, using the specifications established by the Standard Methods for Water and Wastewater (APHA 2012). The color was determined by colorimetry (method 2120B), using a colorimeter (Lovibond PFX 195); Expressing the results in platinum-cobalt units (PCU), turbidity was determined by nephelometry (Method 2130B) using a Turbiquant 3000 IR equipment and mercury (Hg^{2+}) was determined by atomic absorption spectroscopy (AA) in a Thermo Scientific iCE 3300 equipment. Table 1 shows the initial physicochemical characterization values.

Table 1: Initial Physicochemical characterization of wastewater.

Parameters	Value*	Unid
Hg^{2+}	0,036±00	mgL^{-1}
Turbidity	99,45±0,95	NTU
Color	196,4±0,97	PCU
Total Solids	806,0±4,28	mgL^{-1}

* The values represent the mean of three determinations

Equation 1 was used to determine the percentage of adsorbent removal (CA).

$$Removal\ Efficiency\ (\%) = \frac{C_o - C_e}{C_o} * 100 \qquad Eq\ (1)$$

Where, C_o and C_e represent the initial and equilibrium concentration in mg/L.

In addition, the number of mercury ions adsorbed per unit mass of the adsorbent (mg/g) was evaluated using the equation 2 and 3:

$$q_e = \frac{V(C_o - C_e)}{m} \qquad Eq(2)$$

$$q_t = \frac{V(C_o - C_t)}{m} \qquad Eq(3)$$

Where q_e is the number of mercury ions adsorbed at equilibrium per gram of adsorbent in (mg/g), q_t amount of sorbent adsorbed in time t, V is the volume of the test solution (L) and m is the weight of the adsorbent (g) (Hadi et al., 2015). As can be seen in Figure 3a, the removal rate of Hg^{2+} from the solution as a function of time is initially high. According to Attari et al., 2017, this high rate corresponds to the external surface adsorption or boundary layer effect.

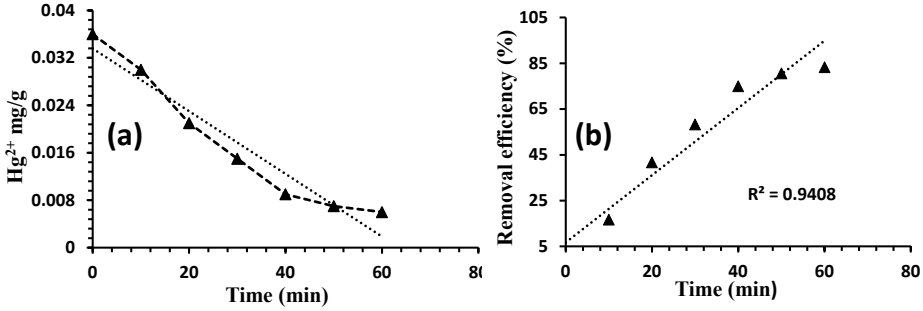

Figure 3: Mercury removal from wastewater. (a) Amount of Hg^{2+} removed as a function of time and(b) Adsorption capacity of CA as a function of time.

Figure 3b shows that the maximum percentage of adsorbent material removal reached 84% and the contact time to reach equilibrium was 60 minutes. The result obtained is very similar to that reported by Boeykens et al. 2019, and Zhao et al., 2020. Who reported percentages of 80 and 89% respectively for the removal of lead and chromium.To explore the mechanism of mercury ion adsorption by CA, two kinetic models and one intraparticle diffusion model were included (Attari et al., 2017; Liu et al., 2020), see Figures 4a-c. According to Attari et al., (2017), in the Elovich kinetic model (Figure 4a), the adsorption kinetics is not affected by the interaction between the adsorbed particles, and when plotting q_t vs ln(t) the value of R^2 must be close to 1. In this case, the value of R^2 was 0.9897, which indicates that the experimental data obtained are very close to the fitted regression line.

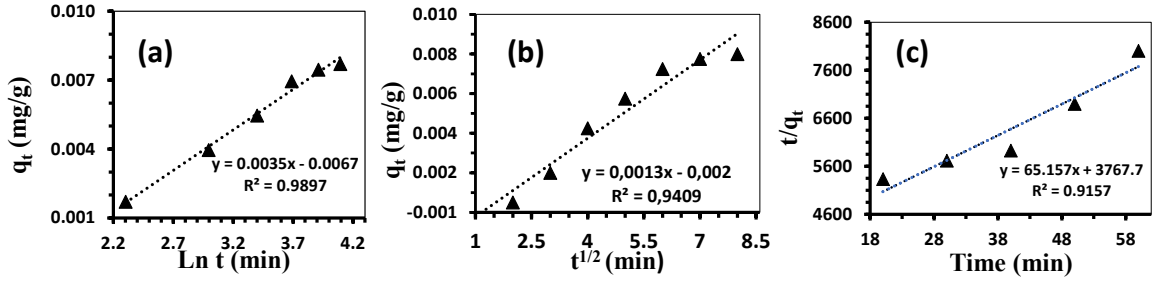

Figure 4: Kinetic models of adsorption of (a) Elovich, (b) Intra-particule difusión and (c) Pseudo-second order.

Intra-particle diffusion (Figure 4b) was expressed according to Weber and Morris (Boparai et al., 2011). The linear graph q_t vs $t^{½}$ should pass through the origin. However, the R^2 value of 0.9409 can be considered a good fit for the regression line. The same happens with the pseudo-second order model whose value of R^2 is 0.9157 (Figure 4c).Table 2 shows the physicochemical characterization of the residual water after treatment with activated carbon, managing to remove turbidity (47.6%), as well as color and total solids; with 57% and 50.2% respectively with values at the 95% level of significance.

Table 2: Physicochemical characterization after treatment with activated carbon.

Parameters	Value	Removal %	Unid
Hg	0,006	83,3 %	mgL^{-1}
Turbidity	52.15 ± 1.2	47,6%	NTU
Color	84.0 ± 1,15	57%	UPC
Total solids	402 ± 2.30	50.2%	mgL^{-1}

The results reported in this study allow us to conclude that the use of *persea americana* "Hass" seeds to obtain carbon and its subsequent activation with orthophosphoric acid, becomes a good alternative to be used in industrial wastewater treatment for Hg^{2+} removal, in addition to reducing turbidity, color and total solids. The maximum rate of adsorption occurs between 10 and 40 minutes, after which the rate decreases until reaching equilibrium between 50 and 60 minutes. The removal rate is mainly due to the fact that most of the active sites are occupied and also to the possible presence of competing ions, such as Na^+, K^+, and Cl^- and to the pH; since at high pH values above 5.0, it is assumed that the formation of mercuric hydroxide occurs.

Acknowledgments

The authors thank the University of Cartagena for their support in carrying out this research, as well as professor Misael Cortes for their valuable contributions

References

Apha, awwa, wef, (22nd ed), 2012, Standard methods for the examination of water and wastewater, Washington.

Attari M, Bukhari S.S, Kazemian H, Rohani S, 2017, A low-cost adsorbent from coal fly ash for mercury removal from industrial wastewater, Journal of environmental chemical engineering, 5, 391–399.

Bibi F., Hussain R., Iqbal N., Saeed S., Waseem M., Elkaeed E. B., Murefah Mana Al-Anazy, Haq S., 2023, Chemical activation and magnetization of onion waste derived carbon for arsenic removal, Arabian journal of chemistry, 16, 105118–105118.

Boeykens S.P., Redondo N., Obeso R.A., Caracciolo N., Vázquez C., 2019, Chromium and lead adsorption by avocado seed biomass study through the use of total reflection x-ray fluorescence analysis, Applied radiation and isotopes, 153, 108809.

Boparai H.K., Joseph M., O'carroll D., 2011, Kinetics and thermodynamics of cadmium ion removal by adsorption onto nano zerovalent iron particles, Journal of hazardous materials, 186, 458–465.

Chen K., Zhang Z., Xia K., Zhou X., Guo Y., Huang T., 2019, Facile synthesis of thiol-functionalized magnetic activated carbon and application for the removal of mercury (II) from aqueous solution, Acs omega, 4, 8568-8579.

Chiarle S., Ratto M., Rovatti M., 2000, Mercury removal from water by ion exchange resins adsorption, Water Research, 34, 2971-2978.

Gheitasi F., Ghammamy S., Zendehdel M., Semiromi F., 2022, Removal of mercury (II) from aqueous solution by powdered activated carbon nanoparticles prepared from beer barley husk modified with thiol/ Fe3O4, Journal of molecular structure, 1267, 33555.

Gluszcz P., Zakrzewska K., Wagner-Doebler I., Ledakowicz S., 2008, Bioreduction of ionic mercury from wastewater in a fixed-bed bioreactor with activated carbon, Chemical paper, 62, 232-238, https://doi.org/10.2478/s11696-008-0017-z

Gupta S., Bhattacharyya K., 2011, Kinetics of adsorption of metal ions on inorganic materials: a review, Advances in colloid and interface science, 162, 39–58, https://doi.org/10.1016/j.cis.2010.12.004

Hadi P., To M., Hui C., Lin C.S.K., Mckay, G., 2015, Aqueous mercury adsorption by activated carbons, Water Research, 73, 37–55.

Lahreche S., Moulefera I., El Kebir A., Sabantina L.; Kaid M.H., Benyoucef A., 2022, Application of activated carbon adsorbents prepared from prickly pear fruit seeds and a conductive polymer matrix to remove congo red from aqueous solutions, Fibers, 10, 7.

Liu Z., Sun Y., Xu X., Qu J., Qu B., 2020, Adsorption of Hg (ii) in an aqueous solution by activated carbon prepared from rice husk using KOH activation, Acs omega, 5, 29231-29242,

Liu Z., Sun Y., Xu X., Meng X., Qu J., Wang Z., Liu C., Qu B., 2020, Preparation, characterization and application of activated carbon from corn cob by KOH activation for removal of Hg (II) from aqueous solution, Bioresource Technology, 306, 123154,

Robati D., 2013, Pseudo-second-order kinetic equations for modeling adsorption systems for removal of lead ions using multi-walled carbon nanotube, Journal of Nanostructure in Chemistry, 3, 1-6.

Rojas J., Gutiérrez E., De Jesús G., 2016, Obtención y caracterización de carbón activado obtenido de lodos de plantas de tratamiento de agua residual de una industria avícola, Ingeniería, investigación y tecnología, 17, 453–462.

Ruiz M., Alexandre M., Fernández C., Gómez V., 2011, Development of activated carbon from vine shoots by physical and chemical activation methods. Some insight into activation mechanisms, Adsorption,17, 621–629.

Samad K., Salleh I., Zahari M., Yussof H., 2019, Batch study on the removal of mercury (II) ion from industrial wastewater using activated palm oil fuel ash, Materials today. Proceedings, 17, 1126–1132.

Viera N., Cruz J., 2019, Influencia de la temperatura de impregnación del azufre sobre el carbón activado de persea american en la adsorción de plomo, hierro y cadmio en soluciones acuosas. Tesis de ingeniería. Universidad nacional de perú.

Zhao J., Yu L., Ma H., Zhou F., Yang K., Wu G., 2020, Corn stalk-based activated carbon synthesized by a novel activation method for high-performance adsorption of hexavalent chromium in aqueous solutions, Journal of Colloid and Interface Science, 578, 650−659.